Nitrogen-induced perturbation of the valence band states in $GaP_{1-x}N_x$ alloys

S. V. Dudiy and Alex Zunger
National Renewable Energy Laboratory, Golden, Colorado 80401, USA

M. Felici, A. Polimeni, and M. Capizzi
CNISM and Dipartimento di Fisica, Università "La Sapienza," Piazzale A. Moro 2, I-00185 Roma, Italy

H. P. Xin and C. W. Tu
Department of Electrical and Computer Engineering, University of California, La Jolla, California 92093, USA
(Received 28 June 2006; published 4 October 2006)

The effects of diluted nitrogen impurities on the valence- and conduction-band states of $GaP_{1-x}N_x$ have been predicted and measured experimentally. The calculation uses state-of-the-art atomistic modeling: we use large supercells with screened pseudopotentials and consider several random realizations of the nitrogen configurations. These calculations agree with photoluminescence excitation (PLE) measurements performed for nitrogen concentrations x up to 0.035 and photon energies up to 1 eV above the GaP optical-absorption edge, as well as with published ellipsometry data. In particular, a predicted nitrogen-induced buildup of the L character near the valence- and conduction-band edges accounts for the surprising broad-absorption plateau observed in PLE between the X_{1c} and the Γ_{1c} critical points of GaP. Moreover, theory accounts quantitatively for the *downward* bowing of the indirect conduction-band edge and for the *upward* bowing of the direct transition with increasing nitrogen concentration. We review some of the controversies in the literature regarding the shifts in the conduction band with composition, and conclude that measured results at ultralow N concentration cannot be used to judge behavior at a higher concentration. In particular, we find that at the *high concentrations* of nitrogen studied here ($\sim 1\%$) the conduction-band edge (CBE) is a hybridized state made from the original GaP X_{1c} band-edge state plus all cluster states. In this limit, the CBE plunges down in energy as the N concentration increases, in quantitative agreement with the measurements reported here. However, at ultralow nitrogen concentrations ($<0.1\%$), the CBE is the nearly unperturbed host X_{1c}, which does not sense the nitrogen cluster levels. Thus, this state does not move energetically as nitrogen is added and stays pinned in energy, in agreement with experimental results.

DOI: 10.1103/PhysRevB.74.155303 PACS number(s): 78.55.Cr, 71.55.Eq, 78.20.Bh

I. INTRODUCTION

GaP is an indirect-gap semiconductor with an X_{1c} conduction-band edge (CBE) located 0.5 eV below the Γ_{1c} direct-band edge. As shown in the 1960s,[1] minute amounts of nitrogen (10^{16} cm^{-3}) can create radiative levels in the gap below the CBE, due either to single-substitutional nitrogen or to nitrogen pairs ("cluster states"), which emit light. Recently, with the advent of molecular-beam epitaxy, it became possible to raise the alloy nitrogen concentration to a few percent (10^{20} cm^{-3}), thus introducing many more nitrogen clusters. This deeply affects the band structure of the material, changing both the discrete cluster-state levels below the CBE and the hostlike X_{1c} and Γ_{1c} band edges.[2–5] Significant spectral changes have also been observed deep inside the conduction band, up to energies exceeding that of the Γ_{1c} direct-gap threshold.[6–10] The "band anticrossing model"[11] was able to explain phenomenologically the shifts in the perturbed hostlike X_{1c} and Γ_{1c} edges. However, it was not able to address (i) the cluster states below the CBE, which dominate photoluminescence spectra, (ii) the evolution of the states between the X_{1c} and Γ_{1c} edges and of the L_{1c}-like states, as determined by photoluminescence excitation[6–8] (PLE) and reflectance[9,10] spectroscopy, or (iii) changes in valence-band states. In contrast, atomistic supercell models[12–18] describe all types of states. Previously, we have shown how such models predict the location of the many N-N pair levels below the CBE, the existence of N-N-N triplet states, their pressure and composition dependence, and the way such cluster states are overtaken by the continuum of perturbed host states once the nitrogen concentration is increased beyond the "amalgamation point."[15–17] None of these effects can be addressed by the two-band anticrossing model. In the present work we direct our attention to the evolution of perturbed host states. In particular, the effects nitrogen incorporation has on the GaPN alloy band states are investigated both theoretically and experimentally. We find that pseudopotential supercell calculations show that the substitution of phosphorus by nitrogen affects also the *valence*-band states, an effect which has been neglected so far. Indeed, the appearance of a plateau in PLE spectra between the X_{1c} band edge and the Γ_{1c} direct edge of GaP can only be accounted for by sizable nitrogen-induced changes of the valence-band states well below the band maximum. The effect of nitrogen on the *conduction* band is described theoretically by calculating the absorption spectra up to energies of ~ 1 eV above the edge. We find that the results depend sensitively on concentration: at the *high concentrations* of nitrogen studied here ($\sim 1\%$) the CBE is a hybridized state made of the original GaP X_{1c} plus all cluster states. In this limit the CBE plunges down in energy as the N concentration increases, in quantitative agreement with the measurements reported here. However, *at the ultralow nitrogen concentra-*

tions considered theoretically in Ref. 17, the CBE is the nearly unperturbed host X_{1c}, which does not sense the localized nitrogen levels. Thus, this state does not move energetically as nitrogen is added, in agreement with the experiments reported in Ref. 19 for nitrogen concentration ranging from 0.008% to 0.1%. Finally, the theoretical prediction[18] of the existence of energy levels associated with N pairs much above the CBE is experimentally supported by the observation in PLE spectra of two weak and otherwise unexplained resonances.

II. METHODS

$GaP_{1-x}N_x$ epilayers were grown by gas-source molecular-beam epitaxy on (001)-oriented GaP substrates. Nitrogen concentrations as determined by x-ray-diffraction measurements range from 0.24% to 3.5%. PLE measurements were taken at low temperature ($T=10$ K) by exciting the samples with a monochromatized tungsten lamp (spectral resolution equal to 2 nm). The luminescence was dispersed by a double 0.75-m-long monochromator and detected by a cooled photomultiplier with a GaAs cathode used in a single-photon-counting mode.

GaPN alloys were modeled by substituting a certain number of anion sites randomly chosen in $(4\times4\times4)$ or $(6\times6\times6)$ GaP supercells with nitrogen atoms. The atomic positions were relaxed by using the valence force-field method.[20] The electronic structure for a given alloy supercell was calculated fully atomistically by means of the empirical pseudopotential method[21] (EPM). Using exactly the same EPM parameters and codes[22,23] as were used previously in Refs. 17 and 18, the characterization of the GaPN random alloy states was extended up to 3.2 eV above the GaP valence-band maximum. We then used the obtained explicit-atomistic wave functions to calculate optical-transition probabilities for transitions from the states in the valence band to those in the conduction band. Transition probabilities are evaluated as dipole-matrix elements squared. To have a quantity that we can compare more directly with PLE intensities, we also calculate the transition probability density as a function of energy ε as

$$P(\varepsilon) \propto \left\langle \sum_{i,j} p_{ij} \tilde{\delta}(\varepsilon - \varepsilon_{ij}) \right\rangle. \quad (1)$$

Here the sum is over different electronic states of the valence and conduction band, indexed by i and j, respectively; ε_{ij} and p_{ij} are the transition energy and probability for an optical transition from state i to state j; $\tilde{\delta}(\varepsilon_{ij})$ is a smeared δ function represented by a Gaussian with some smearing σ; averaging is over different random alloy realizations. This quantity incorporates both the transition probabilities at different energies and the joint density of states, which is important for comparison to PLE data. Note that the present approach is atomistic, in that the supercell is constructed from nitrogen atoms substituting P sites at random. Consequently, each Ga atom can experience different local environments, being coordinated either by 4N, 3N+P, 2N+2P, 1N+3P, or 4 P. This existence of a *distribution* of local environments (each having characteristically different bond length) is a crucial aspect of alloy theory. This feature is missed by the coherent potential approximation, which lets each nitrogen experience but *a single*, "effective" local environment.

III. CLARIFICATION OF PREVIOUS ASSIGNMENTS

Since some of our previous works[17,18,22] have been the subject of misinterpretations,[19,24,25] we summarize in the following those of our main results pertinent to the present discussion.

(i) *The Brillouin zone identity of the conduction band of the alloy system*: Refs. 24 and 25 interpreted previous theoretical work[17,18] to imply that the L_{1c} band of GaP is the alloy state that plunges down in energy as nitrogen atoms are added. However, this is not what the theory proposed. Indeed, because of the absence of long-range order in random substitutional alloys, such as Ga(P,N), their electronic states cannot be described via single-band structure states akin to ordered crystals. Nevertheless, it is possible to decompose the alloy wave function into a *combination* of band states and enquire if there is any wave vector that dominates a given alloy state. This is done by expanding the wave function in a complete set of Bloch functions and summing over bands the projections at a given wave vector (e.g., Γ, L, or X). Here we use such a "majority representation" approach[22] to define and calculate the Γ, L, and X character of each electronic state in the random alloy. The analysis proceeds in terms of *wave vectors* [e.g., (111) being L], not *band states* (e.g., L_{1c}). This means, for example, that contrary to the comments of Refs. 24 and 25 the predominance of the L *character* in the downward-shifting band edge[17] does not imply that this state originates from a single individual L_{1c} *band state*. Indeed, nitrogen perturbation can add a significant L and X admixture even to the electronic states between X_{1c} and L_{1c} critical point energies. In turns, the evolution with N concentration of the higher-energy perturbed host states, such as L_{1c}, cannot be deduced by looking only at the three lowest-energy $\Gamma/L/X$-character states, as suggested by Ref. 24. The evolution of these higher-energy-perturbed host states can be captured, instead, by analyzing the GaPN alloy states over a broad-energy interval of the conduction band.[18] Our calculation shows that the host $a_1(X_{1c})$ and $a_1(L_{1c})$ states should be perturbed by an isolated nitrogen impurity with $a_1(N)$ symmetry more than the $e(X_{1c})$ state. Indeed, the interaction with an isolated nitrogen impurity perturbs and shifts up the $a_1(X_{1c})$ state more than the $e(X_{1c})$ state.[17,18]

(ii) *The different behavior of ultradilute ($x\ll0.1\%$) and more concentrated ($x>0.1\%$) alloys:* Ref. 19 measured the CBE of ultradilute alloys with $x=0.008-0.1\%$, finding that the band edge does not shift with concentration in this range and questioning the results of previous calculations[18] that predicted a precipitous drop in energy of the band-edge state of concentrated alloys, but for higher N concentration ($x\sim1\%$). Indeed, the concentrated regime of $\sim1\%$ nitrogen is characterized by significant nitrogen-nitrogen and nitrogen-host interactions and by the statistical formation of cluster states, thus the band-edge states are well-developed *alloy* states. In particular, in this concentration regime the conduc-

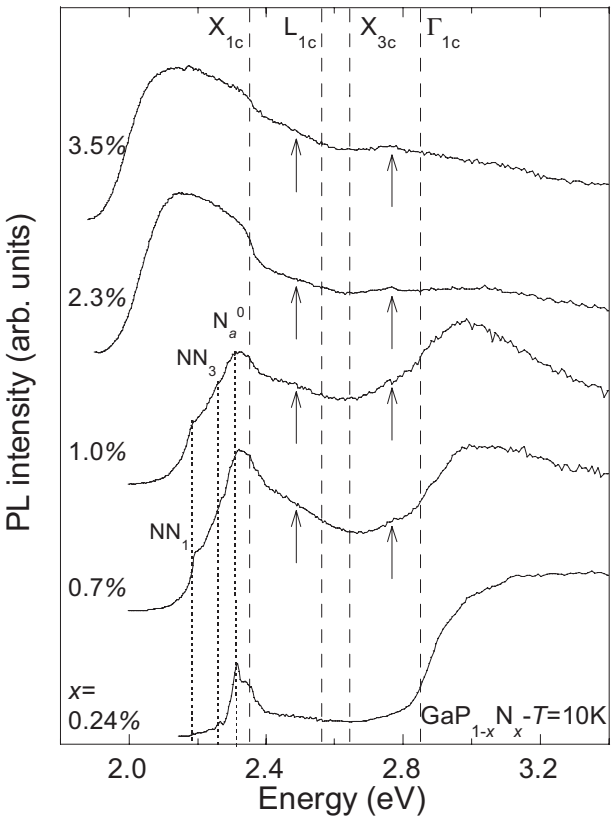

FIG. 1. Photoluminescence excitation spectra of $GaP_{1-x}N_x$ epilayers at $T=10$ K. The short-dashed vertical lines indicate the energy of N single centers and N-related complexes NN_i. The long-dashed vertical lines indicate the energy of GaP critical points. Upward-pointing arrows indicate weak features in the PLE spectra. PLE detection energy is set on the low-energy side of PL spectra.

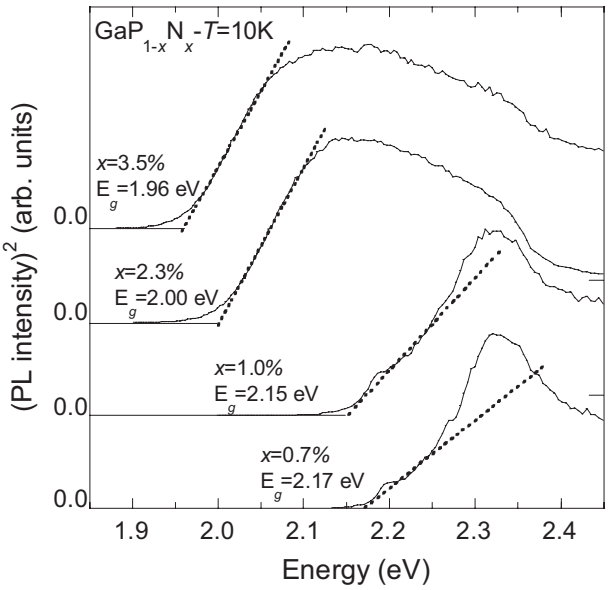

FIG. 2. Fits (dotted lines) of a linear-energy dependence to the square of photoluminescence excitation data in samples with different N concentration, x. The extrapolated values of the effective optical band-gap energy E_g are shown also.

tion band edge is already a hybridized state involving the original GaP X_{1c} state and the nitrogen cluster-state levels. Such a hybridized alloy state—and not the $a_1(X_{1c})$ host state—plunges down in energy as the nitrogen concentration increases and eventually drops below the $e(X_{1c})$ host state, as shown here and in Refs. 17 and 18. As discussed in Ref. 17, such an *alloy* regime is qualitatively different from the ultradilute regime, such as at nitrogen concentrations below 0.1% studied in Ref. 19. In the ultradilute regime the main effect of nitrogen addition is the formation of isolated and hyperlocalized nitrogen states. In that regime the CBE is built predominantly of the perturbed host X_{1c} states with no contribution from the negligible cluster concentration, so no downshift of the CBE is expected even at $x\sim 0.1\%$ [Fig. 19(a) of Ref. 17 and Fig. 1 of Ref. 18]. This is consistent with the experimental findings of Ref. 19.

IV. RESULTS AND DISCUSSION

A. Experiment

The PLE spectra of all investigated samples are shown in Fig. 1. Long-dashed vertical lines indicate the energy positions of the X_{1c}, L_{1c}, X_{3c}, and Γ_{1c} critical points of GaP. The short-dashed vertical lines indicate the energy of the single N state N_a^0, and of N-related complexes NN_i in GaPN, following the notation of Ref. 1. Several features appear in each of the three energy regions of the PLE spectra described in the following: (i) *The energy gap region*. A directlike absorption edge with an exponential Urbach tail increases in intensity and shifts towards lower energy with increasing N concentration x. (ii) *The region between* X_{1c} *and* Γ_{1c} *critical points*. The gap between the X_{1c} and Γ_{1c} critical points is filled up with a weakly structured background until an almost flat plateau develops for $x=2.3\%$ with an intensity larger than that of the Γ_{1c} critical point; see also Refs. 6–8. When the signal is reported on an expanded scale (not shown here), two weak features are found at (2.49 ± 0.05) eV and (2.76 ± 0.01) eV, as indicated by the two upward-pointing arrows. These features can probably be related to the two higher-energy levels of second-nearest-neighbor N pairs (NN_2) predicted at 2.49 and 2.72 eV.[18] Note that out of all states of isolated nitrogen and nitrogen pairs predicted for energies between X_{1c} and Γ_{1c} critical points,[18] those two levels from the second-nearest-neighbor nitrogen pair are practically the only ones that have significant Γ character (Fig. 1 of Ref. 18), and hence the most likely to be visible in PLE. Similar levels predicted for NN_3 pairs (at 2.59 eV) and for NN_4 pairs (at 2.60 eV, quite weak) may also contribute to the oscillator strength buildup observed in this energy region. (iii) *Direct transitions to* Γ_{1c}. The steep increase at the critical Γ_{1c} point (2.85 eV) observed for low N concentration[6–10,26] is smeared out for increasing x until it blurs with the featureless signal at lower energies.

The square of the PLE signal is shown for all but one of the investigated samples in Fig. 2. For high enough N concentrations (when the GaPN alloy-band edge is sufficiently developed), a linear energy dependence $(E\text{-}E_g)$ has been fitted to the low-energy side of the PLE data squared (see dot-

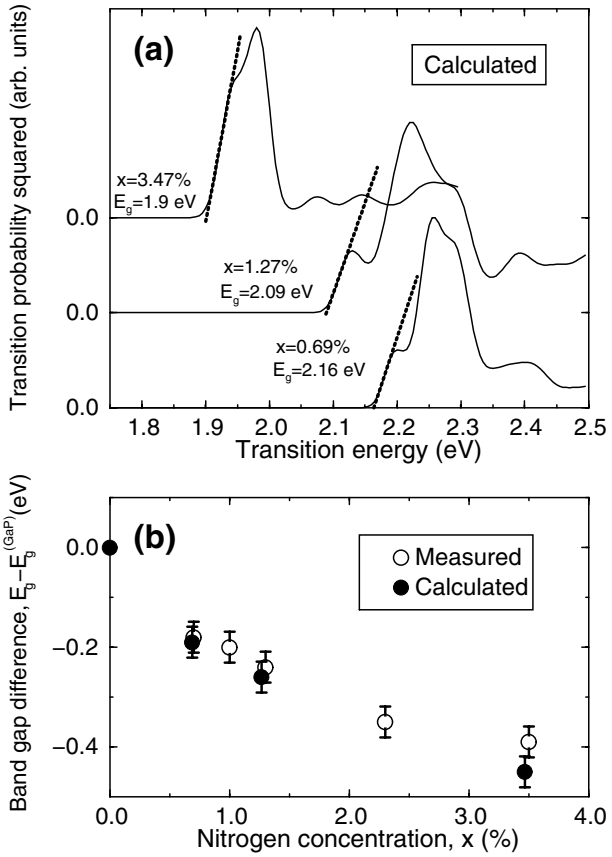

FIG. 3. (a) Calculated energy dependence of the square of the "transition probability" (namely, the dipole-matrix element squared, see text) for optical transitions between the states of the valence- and conduction-band edges in 1728 atom $GaP_{1-x}N_x$ random-alloy supercells. A Gaussian smearing of 0.02 eV is used. Fits of a square-root law (dotted lines) to the calculated dipole matrix squared and values of the extrapolated optical-energy gaps E_g are given. (b) Comparison of the measured values of the shift of E_g as obtained from the fits to the PLE data reported in Fig. 2 (open circles), and from the fits to the theoretically calculated dipole-matrix element squared shown in panel (a) (full dots). The error bars in panel (b) show the uncertainty of the fits in panel (a) and in Fig. 2.

ted lines in the figure). Since we are looking at the emergence of direct transitions [whose oscillator strength is much higher ($\approx 10^3$) than that for indirect transitions (see Ref. 27)], the choice of a square-root law to model the experimental (and calculated) absorption edges appears appropriate. However, we would like to point out that the fitting parameter E_g is a phenomenological parameter to which we will refer in the following as an *effective* optical-band gap. The experimental values of E_g are shown by open circles in Fig. 3(b).

B. Theory

The three different energy ranges investigated experimentally by PLE have been addressed theoretically as follows.

1. Low-energy states below the bulk GaP X_{1c} critical point and band gap bowing

Figure 3(a) shows the intensity for optical-dipole transitions, as defined by Eq. (1), between all states down to 0.3 eV *below* the valence-band maximum and up to 0.3 eV *above* the conduction-band minimum calculated at three different nitrogen concentrations, $x=0.69\%$, 1.27%, and 3.47%. Here the random alloy was simulated in a 1728 atom ($6\times6\times6$) supercell, and the electronic structure results were averaged over 12 random configurations at each x.

Figure 3(a) shows that the calculated conduction-band edge exhibits a clear red shift, broadens, and increases in intensity with increasing x. The *structures* shown in Fig. 3 at an energy higher than that of the effective optical band gap are due to cluster states (CS) measured *below* the conduction band minimum (CBM) in samples with very low nitrogen concentration. These cluster states, which are overtaken by the downward-moving conduction band at higher x,[13] coexist with a broad background whose intensity increases with nitrogen concentration, in agreement with the PLE data shown in Fig. 1. As already reported in Ref. 18, where the bowing coefficient has been analyzed theoretically, the downward-moving conduction band is mostly L-like. The calculated L character does not come from perturbed host L_{1c} states reaching CBM. In fact, the host L_{1c} states actually *move up*, broaden, and decrease in their L character intensity.[18]

We have performed a quantitative comparison between the theoretically calculated and the experimentally measured values of the effective optical band-gap energy [Fig. 3(b)]. The theoretical values of this energy are obtained from a fit of the calculated energy dependence of the transition probability squared to a linear dependence on energy, as done for the experimental data in Fig. 2. These fits are shown by the dotted lines in Fig. 3(a). Figure 3(b) demonstrates good agreement between the theoretical (full dots) and experimental (open circles) results.

Measured PLE spectra in Fig. 1 also show a buildup of intensity, with no noticeable red shift up to about 1%, observed a few tens of meV below X_{1c}. Based on the analysis of the theoretically calculated Γ, L, and X character of electronic states in this energy region,[18] the nonshifting buildup can be attributed to a growing contribution from the increasing number of single nitrogen and nitrogen-cluster states near the GaP X_{1c} energy for increasing N concentration. This is because (i) there is a similar buildup in the calculated Γ, L, and X character, and (ii) the relative magnitudes of the Γ, L, and X character is similar to that of nitrogen-cluster states (a dominance of L and X character).

2. Intermediate energy states between X_{1c} and Γ_{1c} of bulk GaP

Figure 4 shows the calculated density of the dipole-matrix element squared, in the sense of Eq. (1), for transitions from the valence band to the conduction-band states with energies up to the Γ_{1c} critical point and above. In this extended energy range, the inclusion of perturbed valence-band states in the calculations of the dipole-matrix element are presently feasible by performing simulations with 18 random configurations of 4 ($x=1.56\%$) and 9 ($x=3.51\%$) N atoms in 512 atom ($4\times4\times4$) GaPN supercells, at most. In Fig. 4, the dashed lines have been calculated by considering only the Γ-Γ transitions from the three (light, heavy, and split off) valence-band maximum (VBM) states to the conduction-band states ("VBM only" case). The solid lines show, in-

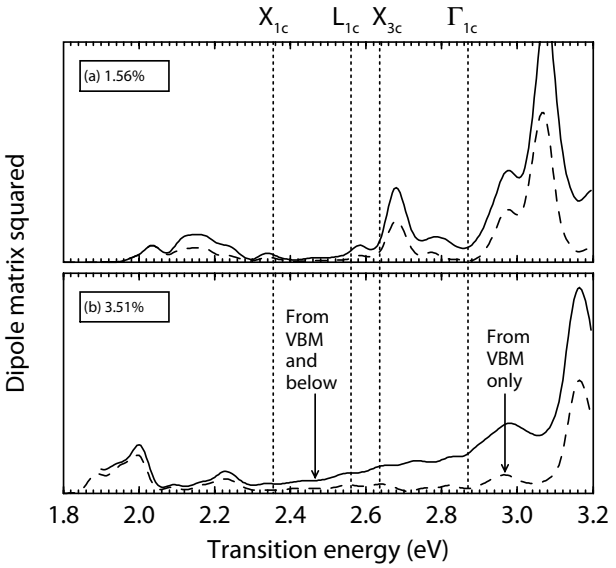

FIG. 4. Calculated energy dependence of the dipole-matrix-element squared density for the case of 18 random-alloy atomic configurations of (a) 4 (x=1.56%) and (b) 9 (x=3.51%) N atoms in a 512 atom ($4\times4\times4$) GaPN supercell. The dashed lines describe the (Γ-Γ) transitions from the three valence-band maximum (VBM) states to the conduction-band states. The solid lines show the energy distribution of the dipole-matrix-element squared density as obtained by including in the above estimate the additional transitions from states below the three VBM states. Gaussian smearing of 0.02 eV is applied. Vertical dashed lines indicate the energies of bulk GaP critical points. The resonance around 2.7 eV in (a) is an artificial supercell-size effect and disappears for larger supercells (e.g., 1728 atom cells in Ref. 18).

stead, the energy dependence of the dipole-matrix element squared as obtained by including transitions from states well below (down to 0.6 eV below) the top of the three valence bands. A Gaussian smearing of 0.02 eV is applied in all these plots.

In the "from VBM only" calculations of Fig. 4 the Γ character of the conduction band in the energy region between the X_{1c} and Γ_{1c} critical points shows a broad, featureless background plateau. Yet, the relative intensity in that region is much lower than that experimentally determined in PLE here, as well as in previous ellipsometry[10] and PLE measurements.[6–8] The agreement between experimental results and theoretical calculations is much better as soon as the role of additional optical transitions from the states below the VBM is taken into account (the solid lines in the figure). We conclude, therefore, that transitions *from below the VBM can contribute significantly to the optical-transition intensity*. This is especially important in the 2.5–3.2 eV region, where a significant buildup of the intensity takes place when the nitrogen concentration increases from 1.56% to 3.51%. This intensity is also relatively broadly spread, though somewhat inhomogeneously, with a bias skewed towards higher energies, a feature consistent with the observed PLE spectra.

We should note that the resonance around 2.7 eV in Fig. 4(a) is an artificial supercell size effect and disappears for larger supercells (e.g., 1728 atom cells in Ref. 18). This artifact reflects insufficiently disordered N arrangements, i.e.,

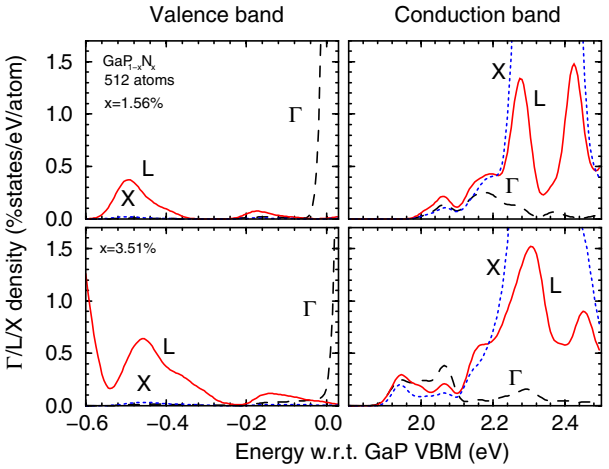

FIG. 5. (Color online) Calculated Γ, L, and X character for N concentrations 1.56% (upper panels) and 3.51% (lower panels) is shown for the valence band (left panels) and for the conduction band (right panels). The eigenstate energies are given with respect to the VBM of pure unstrained GaP, namely, the (weak) VBM bowing is not incorporated. The calculations use 512 atom GaPN ($4\times4\times4$) supercells. The results are averaged over 18 random-alloy configurations, after receiving a Gaussian smearing of 0.02 eV.

too few atoms per supercell. It is important to realize that we can detect such an artifact, which affects only Fig. 4(a) (fewer N atoms case) and appears only for the conduction-band contribution. This feature is narrow in energy and is smeared out as soon as we go to less ordered impurity configurations, namely, by using more N atoms per supercell. We have tested this either by (i) increasing the N concentration while keeping the supercell size fixed [Fig. 4(b)], or (ii)

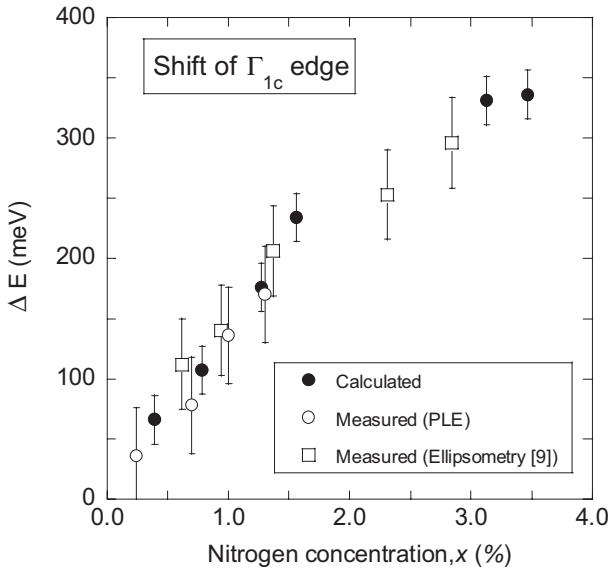

FIG. 6. Energy shift ΔE of the Γ_{1c} critical point as estimated in the present work (full dots) from supercell-empirical pseudopotential calculations for different N concentrations compared to the corresponding shift in the present PLE measurements (open circles) and the shift of the E_0 transition as determined by ellipsometry in Ref. 9 (open squares).

by increasing the supercell size while keeping the N concentration fixed, as in Ref. 18.

The reasons for the increasing intensity of optical transitions from below the VBM are further clarified in Fig. 5 by the analysis of the distribution of Γ, L, and X character over the valence- (left panels) and conduction- (right panels) band edge vicinities. Therein, it can be recognized that the L character builds up near the conduction edge and starting from 0.3–0.4 eV below the valence-band edge and rapidly increases with x, in particular at 0.6 eV below the valence-band maximum. Thus, the featureless PLE background increasing with x in the X_{1c}-Γ_{1c} energy region is due to transitions from below the VBM that are made possible by *the perturbation induced by nitrogen on the valence-band states*, a feature usually overlooked in previous theoretical investigations of III-N-V alloys.

3. High-energy states at and above the GaP Γ_{1c}

Present and previous PLE results, as well as ellipsometry data,[9,10] indicated that the E_0 transition in GaP, from the valence-band states to the Γ_{1c} critical point, moves to higher energies, broadens, and gradually disappears with increasing x. This qualitative behavior is well described by our theoretical method.[18] In addition, the shift of the Γ_{1c} critical point with nitrogen concentration is well reproduced by the present calculations. This is shown in Fig. 6, where theoretical results for the energy of the E_0 transition (full dots) agree rather well with the values experimentally determined by PLE in the present work (open circles) and by ellipsometry in Ref. 9 (open squares).

V. CONCLUSIONS

Present and previous PLE measurements on GaPN epilayers having nitrogen concentration up to 3.5% have been compared with large-supercell empirical pseudopotential calculations of the electronic structures of random alloys. The large-supercell calculations reproduce the main features observed in the PLE spectra and provide new insights into the nature of those features. In particular, the calculations account quantitatively for the downward-moving conduction-band edge, and qualitatively for the increasingly large Γ character of this edge. Moreover, a PLE background increasing with nitrogen concentration between the GaP X_{1c} and Γ_{1c} critical points is explained by taking into account transitions from below the valence-band maximum, which are strongly affected by N insertion in the lattice. Similarly, some weak features observed in the PLE spectra in this energy region might be identified with excited levels of second-nearest-neighbor nitrogen pairs resonant with the conduction-band states, as predicted in Ref. 18. Finally, the blueshift and broadening of the Γ_{1c} critical point observed in previous PLE and ellipsometry measurements is qualitatively and quantitatively accounted for.

ACKNOWLEDGMENT

Work at NREL is supported by the U.S. Department of Energy, SC-BES-DMS Grant No. DEAC36-98-GO10337.

[1] D. G. Thomas, J. J. Hopfield, and C. J. Frosch, Phys. Rev. Lett. **15**, 857 (1965).
[2] S. Miyoshi, H. Yaguchi, K. Onabe, R. Ito, and Y. Shiraki, Appl. Phys. Lett. **63**, 3506 (1993).
[3] H. P. Xin, C. W. Tu, Y. Zhang, and A. Mascarenhas, Appl. Phys. Lett. **76**, 1267 (2000).
[4] Y. Zhang, B. Fluegel, A. Mascarenhas, H. P. Xin, and C. W. Tu, Phys. Rev. B **62**, 4493 (2000).
[5] I. A. Buyanova, G. Pozina, J. P. Bergman, W. M. Chen, H. P. Xin, and C. W. Tu, Appl. Phys. Lett. **81**, 52 (2002).
[6] H. Yaguchi, S. Miyoshi, G. Biwa, M. Kibune, K. Onabe, Y. Shiraki, and R. Ito, J. Cryst. Growth **170**, 353 (1997).
[7] I. A. Buyanova, M. Izadifard, W. M. Chen, H. P. Xin, and C. W. Tu, Phys. Rev. B **69**, 201303(R) (2004).
[8] M. Felici, A. Polimeni, M. Capizzi, S. V. Dudiy, A. Zunger, I. A. Buyanova, M. W. Chen, H. P. Xin, and C. W. Tu, in *Proceedings of the 27th International Conference on the Physics of Semiconductors, Flagstaff 2004*, edited by J. Menéndez and C. G. Van de Walle (American Institute of Physics, New York, 2005), p. 265.
[9] G. Leibiger, V. Gottschalch, M. Schubert, G. Benndorf, and R. Schwabe, Phys. Rev. B **65**, 245207 (2002).
[10] H. Kanaya, H. Yaguchi, Y. Hijakata, S. Yoshida, S. Miyoshi, and K. Onabe, Phys. Status Solidi C **0**, 2753 (2003).
[11] W. Shan, W. Walukiewicz, K. M. Yu, J. Wu, J. W. Ager III, E. E. Haller, H. P. Xin, and C. W. Tu, Appl. Phys. Lett. **76**, 3251 (2000).
[12] L. Bellaiche, S.-H. Wei, and A. Zunger, Phys. Rev. B **54**, 17568 (1996); **56**, 10233 (1997).
[13] T. Mattila, L.-W. Wang, and A. Zunger, Phys. Rev. B **59**, 15270 (1999).
[14] P. R. C. Kent and A. Zunger, Phys. Rev. Lett. **86**, 2613 (2001).
[15] P. R. C. Kent and A. Zunger, Appl. Phys. Lett. **79**, 2339 (2001).
[16] P. R. C. Kent and A. Zunger, Appl. Phys. Lett. **82**, 559 (2001).
[17] P. R. C. Kent and A. Zunger, Phys. Rev. B **64**, 115208 (2001).
[18] S. V. Dudiy, P. R. C. Kent, and A. Zunger, Phys. Rev. B **70**, 161304(R) (2004).
[19] B. Fluegel, Y. Zhang, J. F. Geisz, and A. Mascarenhas, Phys. Rev. B **72**, 073203 (2005).
[20] P. Keating, Phys. Rev. **145**, 637 (1966).
[21] K. Kim, P. R. C. Kent, A. Zunger, and C. B. Geller, Phys. Rev. B **66**, 045208 (2002).
[22] L.-W. Wang, L. Bellaiche, S.-H. Wei, and A. Zunger, Phys. Rev. Lett. **80**, 4725 (1998).
[23] L.-W. Wang and A. Zunger, J. Chem. Phys. **100**, 2394 (1994).
[24] Y. Zhang, B. Fluegel, M. C. Hanna, J. F. Geisz, L.-W. Wang, and A. Mascarenhas, Phys. Status Solidi B **240**, 396 (2003).
[25] B. Fluegel, Y. Zhang, J. F. Geisz, and A. Mascarenhas, APS March Meeting (2005).
[26] M. Felici, A. Polimeni, A. Miriametro, M. Capizzi, H. P. Xin, and C. W. Tu, Phys. Rev. B **71**, 045209 (2005).
[27] F. Bassani and P. Parravicini, *Electronic States and Optical Transitions in Solids* (Pergamon Press, Oxford, 1975), p. 168.